

Blends of Nylon 6 with an Ethylene-Based Multifunctional Polymer. II.

Property–Morphology Relationships

HSIAO-KEN CHUANG and CHANG DAE HAN, *Department of Chemical Engineering, Polytechnic Institute of New York, Brooklyn, New York 11201*

Synopsis

The tensile properties and impact strength were measured of the three blend systems, nylon 6/CXA 3101, nylon 6/Plexar 3, and nylon 6/EVA, which had been prepared using a twin-screw compounding machine. Scanning electron micrographs (SEM) of the fracture surfaces show that the domain size of the dispersed phase is much smaller in the nylon 6/CXA 3101 blends or nylon 6/Plexar 3 blends than in the nylon 6/EVA blends. This is attributed to the presence of a graft copolymer, formed by chemical reactions between carboxyl or anhydride groups present in the CXA 3101 (or Plexar 3) and the amino end groups of the nylon 6, at the boundaries of the dispersed and continuous phases. The SEM analysis of the fracture surfaces shows that no discrete particles are exposed on the fracture surface of either the nylon 6/CXA 3101 blends or nylon 6/Plexar 3 blends, supporting the theory that a graft copolymer, formed during melt blending, helped the discrete particles adhere to the continuous matrix.

INTRODUCTION

In heterogeneous polymer blends, there are many interrelated variables which affect the mechanical/physical properties of the finished product. Such interrelationships are displayed schematically in Figure 1. For instance, the method of blend preparation (i.e., the method of mixing the polymers and the intensity of mixing) controls the morphology of the blend (i.e., the state of dispersion, domain size, and its distribution), which in turn controls the rheological properties of the blend. On the other hand, the rheological properties strongly dictate the choice of processing conditions (e.g., temperature, shear stress), which in turn strongly influence the morphology and, therefore, the mechanical/physical properties of the finished product. Such intricate interrelationships in heterogeneous polymer blend systems have been demonstrated in a recent monograph by Han.¹

The intensity of shear or elongation deformation, while either preparing a blend (i.e., compounding) or fabricating an already compounded blend, profoundly influences the morphological state of the fabricated product. For instance, Han and Kim² demonstrated that, in the melt spinning of blends of high-density polyethylene (HDPE) and polystyrene (PS) that formed two phases in the molten state, the ratio of the elongational viscosities of the constituent components dictated the shape of the dispersed phase in the melt-spun fiber. Specifically, when the dispersed phase in the HDPE/PS blends had an elongational viscosity lower than the continuous phase, the

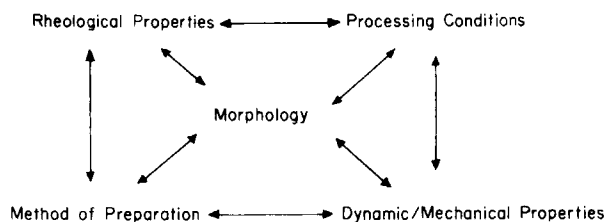


Fig. 1. Schematic depicting the structure-property-morphology relationships in dispersed polymer blend systems.

dispersed phase was elongated considerably during the spinning operation (i.e., under elongational flow). It can be easily surmised that the shape of the dispersed phase in a heterogeneous blend influences the resultant end-use mechanical properties. Indeed, Han¹ has shown that, when the dispersed phase formed long threadlike shapes in the melt-spun fibers of HDPE/PS blends, the resultant fibers showed reinforcement.

In the injection molding operation, mold flow is often sufficient to produce a significant orientation of the dispersed phase suspended in the continuous phase. The breaking up of the domains at high strain rates and the accompanying reorientation, of course, minimize the original orientation effects. Asar et al.,³ for instance, reported that the impact properties of an injection-molded blend of polypropylene (PP) and ethylene-propylene-diene terpolymer (EPDM) depend on the blend composition and processing variables. They observed that local variations in the EPDM concentration and the domain size resulted in a twofold difference in the total energy absorbed during impact. This indicates clearly that the injection molding conditions, which in turn control the morphology (i.e., the distribution of the EPDM) and the domain size, have a profound influence on the mechanical properties of heterogeneous polymer blends.

Having presented in Part I of this series⁴ the rheology-structure relationships of the three blend systems investigated, namely, nylon 6/CXA 3101 blends, nylon 6/Plexar 3 blends, and nylon 6/EVA blends, we shall present in this paper the property-morphology relationships of these blend systems. More specifically, we shall present the analysis of fracture tests to elucidate the mechanism of fracture observed in our study at the microscopic level. Fracture surfaces were investigated by electron microscopy, and both tensile properties and impact strength of the injection-molded specimens were measured. Emphasis will be placed on the importance of the presence of an *interphase* at the polymer-polymer boundaries in improving the mechanical properties of heterogeneous polymer blends.

EXPERIMENTAL

We have used the following three blend systems: (1) nylon 6/CXA 3101, (2) nylon 6/Plexar 3, and (3) nylon 6/EVA. Sample codes and the method used for preparing these blend systems are already described in Part I of this series.⁴

For the purpose of the present investigation, the melt-blended pellets were injection-molded to obtain test specimens for the measurement of

tensile properties and Izod impact strength. Before their use, the test specimens were vacuum dried at 70°C for 30 h to remove moisture and to relieve the frozen-in stress. The dried test specimens were stored in a dessicator until use.

Tensile property measurements were done on an Instron machine at room temperature following the procedure described in ASTM D638. A crosshead speed of 0.508 cm/min was used in all measurements.

All the specimens for the Izod impact strength measurement had the dimensions 6.35 cm × 1.27 cm × 0.317 cm, with a notch 0.0254 cm in radius. The notched Izod impact strength was measured, using a Baldwin impact testing machine at room temperature.

The Izod impact fracture surface and the tensile fracture surface of the test specimens were studied, using a scanning electron microscope (SEM) (AMR 1200) operated at 15–25 kV. The surfaces of the tensile and impact fracture specimens were coated with gold to avoid charging under an electron beam.

RESULTS AND DISCUSSION

Tensile Properties and Phase Morphology

The stress–strain curves are shown in Figure 2 for the nylon 6/CXA 3101 blends, in Figure 3 for the nylon 6/Plexar 3 blends, and in Figure 4 for the nylon 6/EVA blends. It is seen in Figures 2–4 that the nylon-rich blends in

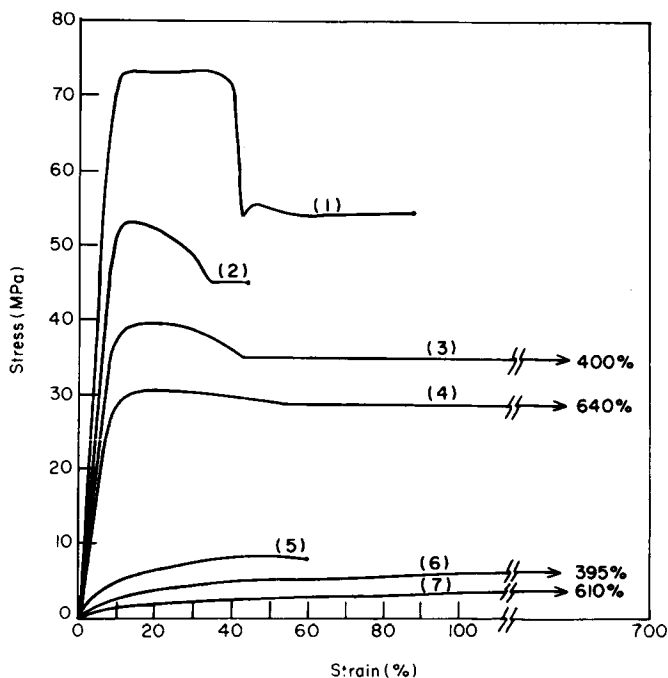


Fig. 2. Stress–strain curves for the nylon 6/CXA 3101 blend system: (1) nylon 6; (2) nylon 6/CXA 3101 = 80/20; (3) nylon 6/CXA 3101 = 60/40; (4) nylon 6/CXA 3101 = 50/50; (5) nylon 6/CXA 3101 = 40/60; (6) nylon 6/CXA 3101 = 20/80; (7) CXA 3101.

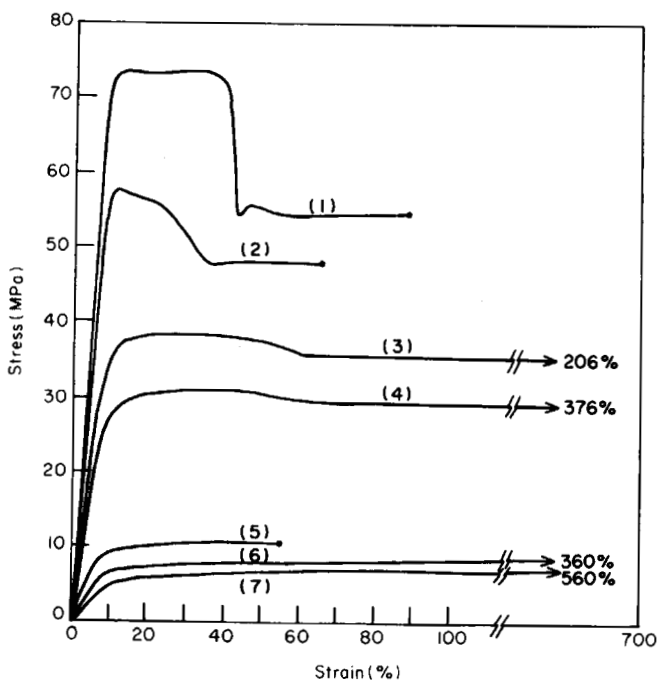


Fig. 3. Stress-strain curves for the nylon 6/Plexar 3 blend system: (1) nylon 6; (2) nylon 6/Plexar 3 = 80/20; (3) nylon 6/Plexar 3 = 60/40; (4) nylon 6/Plexar 3 = 50/50; (5) nylon 6/Plexar 3 = 40/60; (6) nylon 6/Plexar 3 = 20/80; (7) Plexar 3.

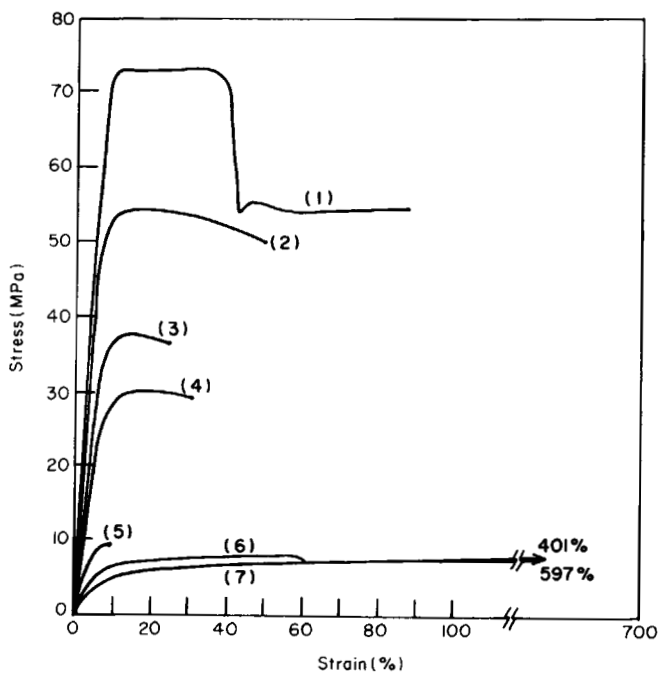


Fig. 4. Stress-strain curves for the nylon 6/EVA blend system; (1) nylon 6; (2) nylon 6/EVA = 80/20; (3) nylon 6/EVA = 60/40; (4) nylon 6/EVA = 50/50; (5) nylon 6/EVA = 40/60; (6) nylon 6/EVA = 20/80; (7) EVA.

the nylon 6/CXA 3101 and nylon 6/Plexar 3 blend systems undergo extensive yielding and necking, whereas the nylon-rich blends in the nylon 6/EVA blend system do not. We believe that this difference is due to the fact that the large domain size of the dispersed EVA particles in the nylon/EVA blends, as will be shown below in SEM micrographs, interrupted the change of the folded-chain structure of the nylon 6 to form a fibrillar (i.e., extended) morphology, oriented in the direction of stretching. In other words, depending upon the morphological state of the nylon 6, forming the continuous phase in the nylon-rich blends, different stress-strain behaviors are observed. When spherulites are present in specimens of the nylon 6/CXA 3101 and nylon 6/Plexar 3 blends, tensile tests indicate ductility and a tendency toward cold-drawing.

The tensile modulus versus blend composition curves are shown in Figure 5 for the nylon 6/CXA 3101 blends, in Figure 6 for the nylon 6/Plexar 3 blends, and in Figure 7 for the nylon 6/EVA blends. In these figures, theoretical predictions of the tensile modulus, based the theories suggested in the literature,^{5,6} are also given. Since the mechanical properties of heterogeneous polymer blends are dependent upon the microstructure of the specimens, we will first discuss the morphology of the fracture surface of the blend specimens investigated and then review the theories used in Figures 5-7.

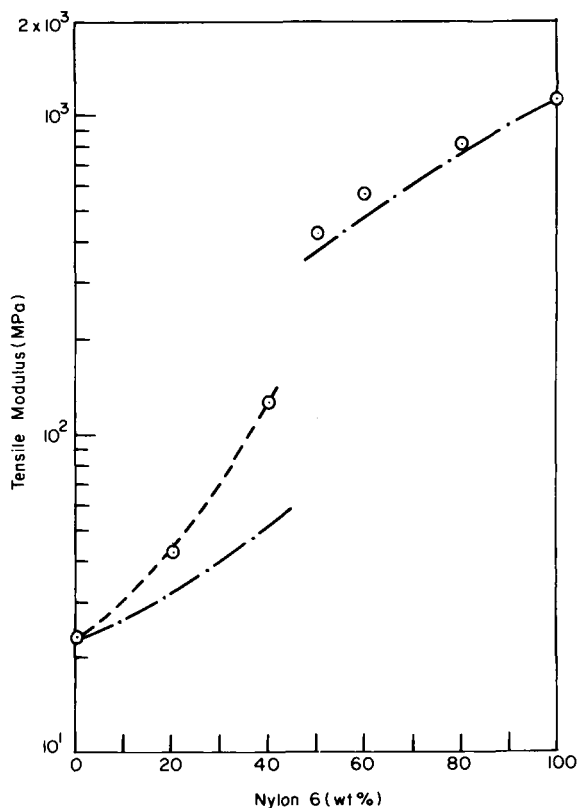


Fig. 5. Tensile modulus vs. blend composition for the nylon 6/CXA 3101 blend system: (⊙) experimental data; (— · —) Kerner's model; (- - -) Nielsen's model.

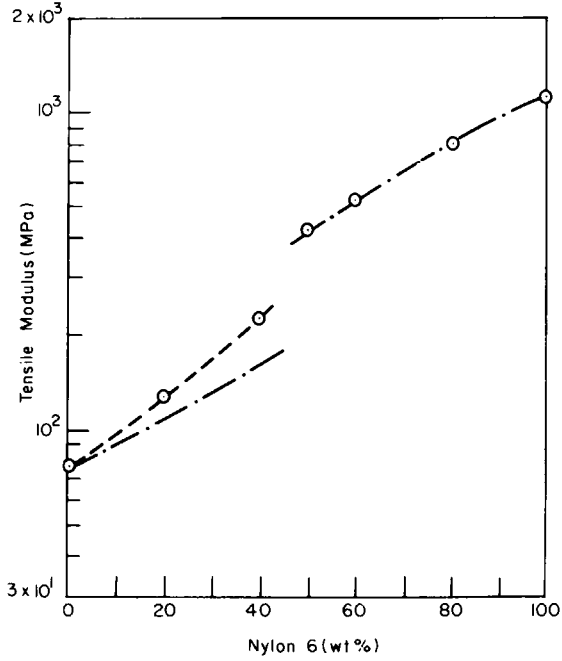


Fig. 6. Tensile modulus vs. blend composition for the nylon 6/Plexar 3 blend system: (○) experimental data; (— · —) Kerner's model; (- - -) Nielsen's model.

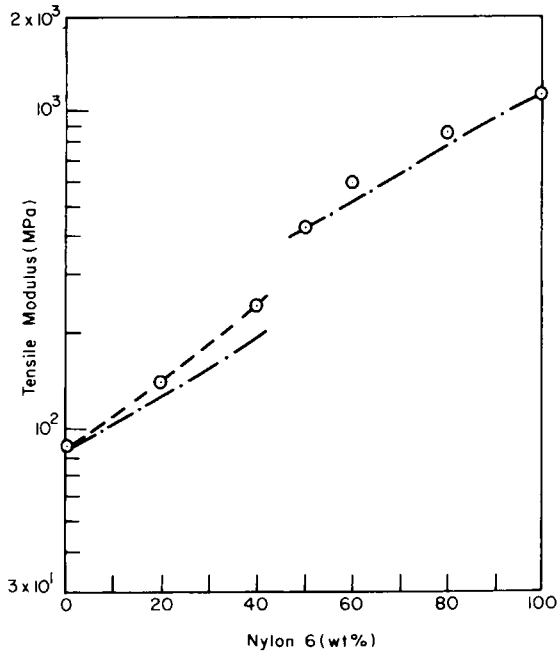


Fig. 7. Tensile modulus vs. blend composition for the nylon 6/EVA blend system: (○) experimental data; (— · —) Kerner's model; (- - -) Nielsen's model.

The SEM micrographs of the tensile fracture surface of the nylon-lean blends are given in Figure 8 for the nylon 6/CXA 3101 blend system, in Figure 9 for the nylon 6/Plexar 3 blend system, and in Figure 10 for the nylon 6/EVA blend system. It is seen in Figure 8 that the nylon particles are not exposed on the fracture surface and that the dispersed nylon particles are covered by a layer of another polymer. This seems to indicate that an interfacial adhesion exists between the dispersed phase (nylon particles) and the continuous phase (CXA 3101 matrix). On the other hand, Figure 10 shows clearly that the dispersed phase are exposed on the fracture surface, giving little evidence of interfacial adhesion between the dispersed phase (nylon particles) and the continuous phase (EVA matrix). Figure 9 shows that the extent of interfacial adhesion in the nylon 6/Plexar 3 blend system lies somewhere between that in the nylon 6/CXA 3101 blend system and that in the nylon 6/Plexar 3 blend system.

It should be mentioned at this juncture that, since SEM micrographs could not distinguish which of the two constituent components forms the discrete and which the continuous phase, we have used phase-contrast optical microscopy to answer this question. We confirmed that, in the nylon-lean blends considered in Figures 8–10, rigid nylon particles are dispersed in the soft continuous matrix (i.e., CXA 3101, Plexar 3, or EVA), and that in the nylon-rich blends, soft particles of CXA 3101 (or Plexar 3 or EVA)

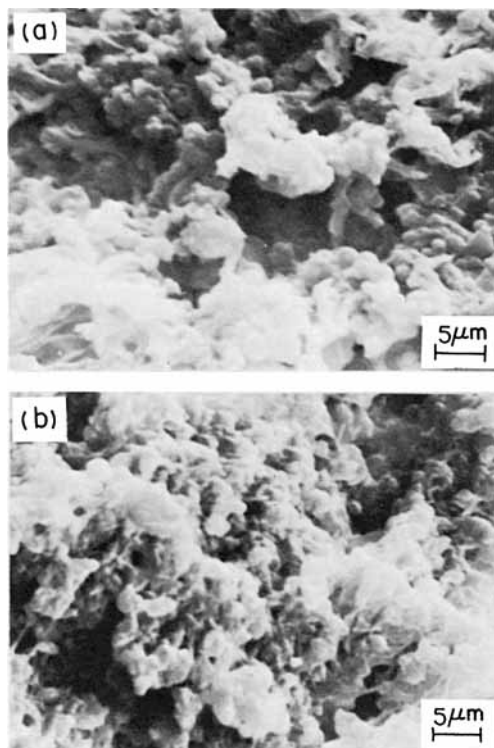


Fig. 8. SEM micrographs of the tensile fracture surface of: (a) nylon 6/CXA 3101 = 40/60 blend; (b) nylon 6/CXA 3101 = 20/80 blend.

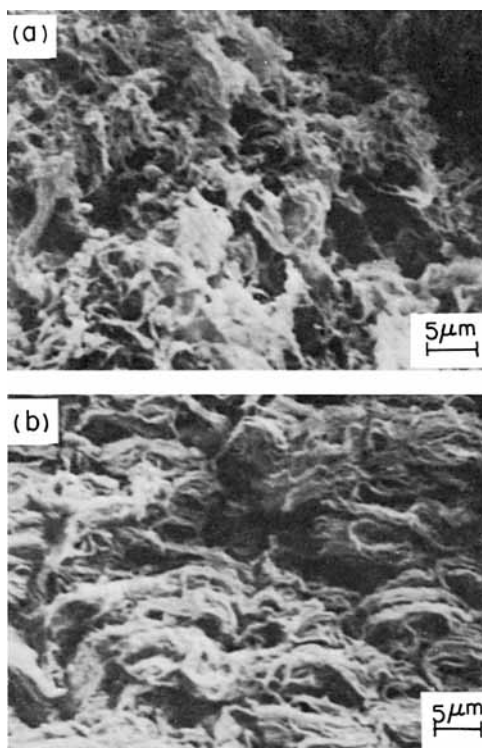


Fig. 9. SEM micrographs of the tensile fracture surface of: (a) nylon 6/Plexar 3 = 40/60 blend; (b) nylon 6/Plexar 3 = 20/80 blend.

are dispersed in the rigid nylon matrix, as may be seen in the SEM micrographs given in Figures 11–13. Note that in Figure 11 no dislodging of soft CXA 3101 particles is noticeable on the fracture surface in the nylon 6/CXA 3101 blends, whereas in Figure 13 soft EVA particles are exposed on the fracture surface in the nylon 6/EVA blends.

As discussed in Part I of this series,⁴ we believe that, in the nylon 6/CXA 3101 blends, chemical reactions have taken place between carboxyl or anhydride groups present in the CXA 3101 and the amino end groups of the nylon 6, forming a graft copolymer. As pointed out by Illing,⁷ a graft copolymer thus formed stays preferentially on the surface of the dispersed particles, acting as an “interfacial agent.” The presence of such an interfacial agent would require less energy needed for breaking large dispersed particles during melt blending, and thus would give rise to smaller domains of the discrete phase strongly adherent to the continuous phase. On the other hand, as may be seen clearly in Figures 10 and 13, there is little or no evidence of adhesion between the nylon 6 particles and the EVA matrix in the nylon 6/EVA blends. This is not surprising in view of the fact that the EVA has no functional group that could react chemically with amino end groups of nylon 6.

Let us now turn to the theoretical predictions of the tensile modulus of heterogeneous polymer blends. Among the several theories reported in the literature,^{5,6,8–11} we have considered the following two models, namely, the

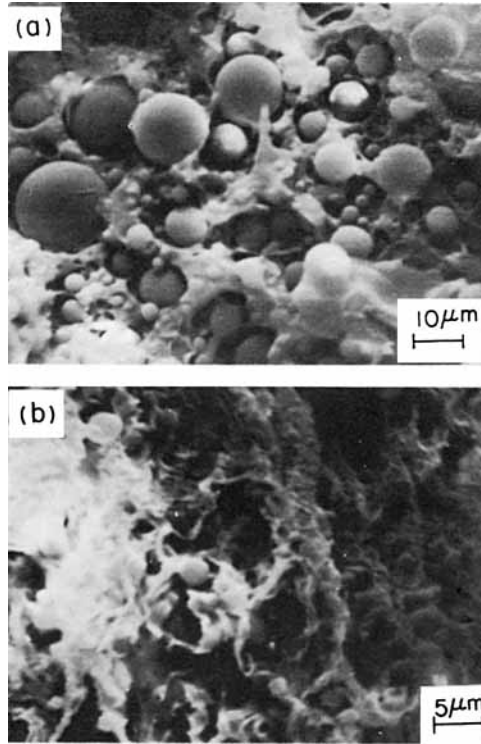


Fig. 10. SEM micrographs of the tensile fracture surface of: (a) nylon 6/EVA = 40/60; (b) nylon 6/EVA = 20/80.

Kerner model⁵ and the Nielsen model.⁶ We realize that the Kerner model was originally developed for the shear modulus of a composite containing spherical solid particles, with the assumption that both the matrix and the inclusions (i.e., suspended particles) have the same Poisson's ratio, 0.5. In the blend systems we investigated, the Poisson's ratios of nylon 6 and CXA 3101 (Plexar 3 or EVA) are 0.44 and 0.5, respectively. We felt that these values are close enough to justify the use of the Kerner model to predict the tensile modulus of the specimens tested.

For a system having perfect adhesion at the phase boundary, the Kerner model may be written as⁵

$$E_b = E_m \left[\frac{\Phi_d E_d}{(7 - 5\nu_m)E_m + (8 - 10\nu_m)E_d} + \frac{\Phi_m}{15(1 - \nu_m)} \right] \left[\frac{\Phi_d E_m}{(7 - 5\nu_m)E_m + (8 - 10\nu_m)E_d} + \frac{\Phi_m}{15(1 - \nu_m)} \right] \quad (1)$$

where E is the tensile modulus, Φ is the volume fraction, and ν is Poisson's ratio. The subscripts b , m , and d refer to the blend, the matrix, and the dispersed phase, respectively.

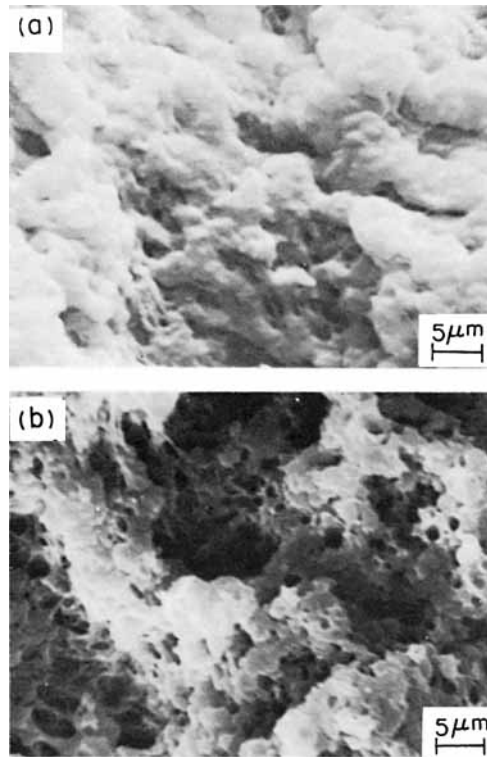


Fig. 11. SEM micrographs of the tensile fracture surface of: (a) nylon 6/CXA 3101 = 80/20; (b) nylon 6/CXA 3101 = 60/40.

It should be pointed out that the Kerner model may not be applicable to polymer blend systems in which strong interactions between the inclusions and the matrix may exist, because it assumes that the influence of the inclusions extends through only a limited region of the matrix. For such situations, Nielson⁶ suggested a modification of the Kerner model. According to Nielson,⁶ we have the following expressions.

(i) For a rigid polymer dispersed in a soft matrix,

$$\frac{E_b}{E_m} = \frac{1 + AB\Phi_d}{1 - B\Psi\Phi_d} \quad (2)$$

in which

$$B = \left(\frac{E_d}{E_m} - 1 \right) \left/ \left(\frac{E_d}{E_m} + A \right) \right., \quad \Psi = 1 + \left(\frac{1 - \Phi_{\max}}{(\Phi_{\max})^2} \right) \Phi_d \quad (3)$$

(ii) For soft inclusions in a rigid matrix,

$$\frac{E_m}{E_b} = \frac{1 + AC\Phi_d}{1 - C\Psi\Phi_d} \quad (4)$$

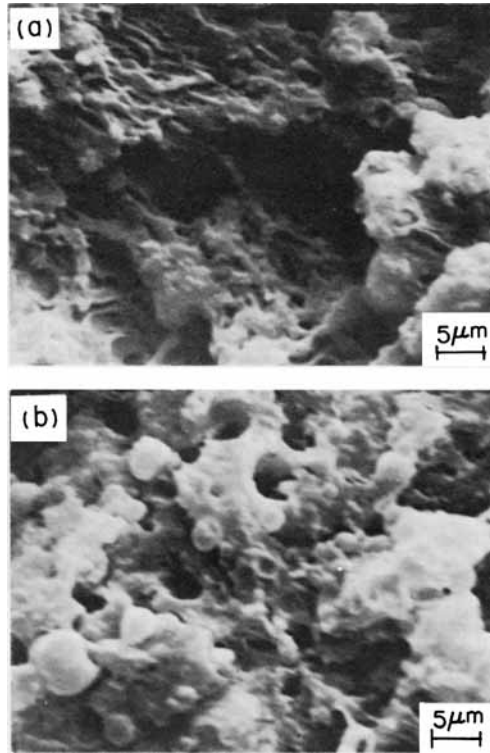


Fig. 12. SEM micrographs of the tensile fracture surface of: (a) nylon 6/Plexar 3 = 80/20; (b) nylon 6/Plexar 3 = 60/40.

in which

$$C = \left(\frac{E_m}{E_d} - 1 \right) \left/ \left(\frac{E_m}{E_d} + A \right) \right., \quad \Psi = 1 + \left(\frac{1 - \Phi_{\max}}{(\Phi_{\max})^2} \right) \Phi_d \quad (5)$$

Note that Φ_{\max} in eqs. (3) and (5) denotes the maximum packing volume which can be considered as a scale of the interactions between the two phases. A small value of Φ_{\max} represents a large extent of adherent interphase, which is immobilized by the inclusions. The constant A in eqs. (2) and (4) takes into account the geometry of the particulate phase. For spherical particles in a two-phase system that have the same Poisson's ratio for both the suspended particles and suspending medium, the constant A in eq. (2) may be represented by $(7 - 5\nu_m)/(8 - 10\nu_m)$ and the constant A in eq. (4) by $(8 - 10\nu_m)/(7 - 5\nu_m)$. Equations (1), (2), and (4) were used to predict the theoretical values of tensile modulus shown in Figures 5-7.

It is seen that eq. (1) fits the experimental data of nylon-rich blends rather well, but it does not do a good job for nylon-lean blends. On the other hand, eq. (2) was used to fit the experimental data by adjusting the parameter Φ_{\max} . The values of Φ_{\max} used for the blend systems investigated are listed in Table I. The domain size of the discrete phase in each of the blends was estimated from the tensile fracture micrographs shown in Figures 8-10. It

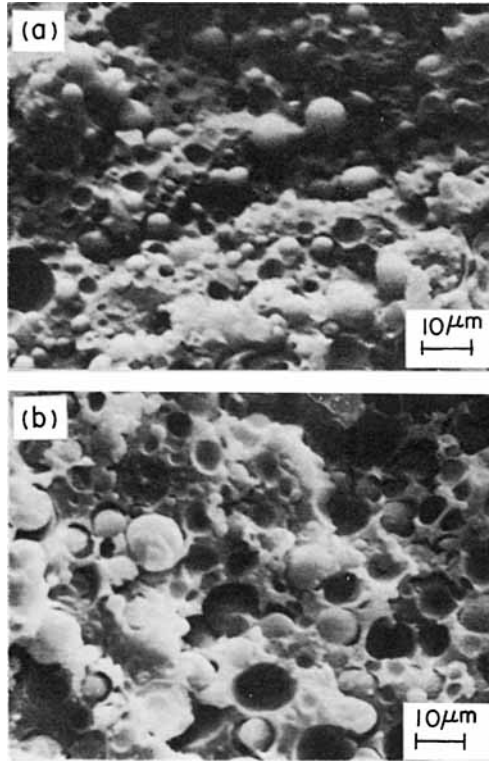


Fig. 13. SEM micrographs of the tensile fracture surface of: (a) nylon 6/EVA = 80/20; (b) nylon 6/EVA = 60/40.

is seen in Table I that Φ_{\max} values of the nylon 6/EVA blends are greater than those of the nylon 6/Plexar 3 blends, which, in turn, are greater than those of the nylon 6/CXA 3101 blends. Note that the reciprocal of Φ_{\max} may be considered as a measure of the thickness of the interphase. Therefore, it can be said qualitatively that the thickness of the interphase of the three blend systems investigated has the following order: nylon 6/CXA 3101

TABLE I
Maximum Packing Volume and Domain Size of the Nylon-Lean Blends

Blend composition (by weight)	Maximum packing volume fraction Φ_{\max}	Domain size (μm)
Nylon 6/CXA 3101 = 40/60	0.418	0.3-2.5
Nylon 6/CXA 3101 = 20/80	0.327	0.5-1.5
Nylon 6/Plexar 3 = 40/60	0.523	1.0-3.5
Nylon 6/Plexar 3 = 20/80	0.430	0.5-1.5
Nylon 6/EVA = 40/60	0.750	0.5-10.0
Nylon 6/EVA = 20/80	0.670	0.5-5.0

blends > nylon 6/Plexar 3 blends > nylon 6/EVA blends. Compared to the well-developed theories for predicting the modulus of polymer blends, relatively little is available for theoretically predicting the tensile strength of polymer blends. According to Kunori and Geil¹² and Nielsen,⁶ the tensile failure of a blend is attributable to the failure of the adhesion between the discrete phase and the continuous phase, through crazing or a dewetting effect. The crazing or void depends on the area occupied by the discrete phase in the blend.

The tensile strengths of the blend systems investigated are shown in Figure 14. It is seen that in the nylon-rich blends having nylon 6 as the continuous phase, the tensile strength decreases monotonically as the amount of nylon 6 in a blend is decreased. In the nylon-lean blends having nylon 6 as the discrete phase, however, the tensile strengths of the nylon 6/CXA 3101 blends (or nylon 6/Plexar 3 blends) stay almost constant as the amount of nylon 6 increases. On the other hand, the tensile strength of the nylon 6/EVA blends goes through a minimum, indicating little or no adhesion between the dispersed nylon particles and the continuous EVA matrix.

The elongation at break is given in Figure 15 as a function of blend composition. It is seen that in the nylon-rich blends containing 50 and 60 wt % of nylon 6, respectively, the elongation at break of the nylon 6/CXA

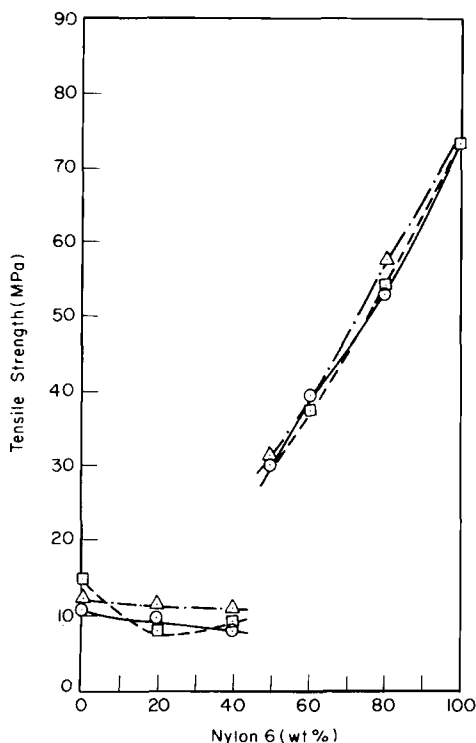


Fig. 14. Tensile strength vs. blend composition for: (○) nylon 6/CXA 3101 blend system; (△) nylon 6/Plexar 3 blend system; (□) nylon 6/EVA blend system.

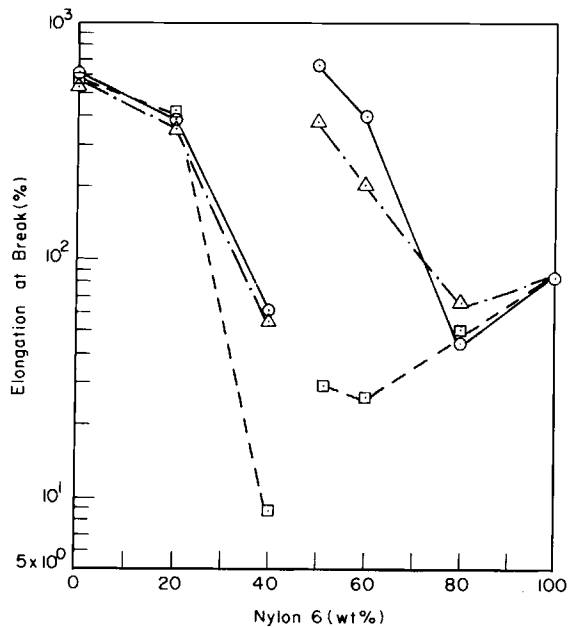


Fig. 15. Percent elongation vs. blend composition for: (○) nylon 6/CXA 3101 blend system; (△) nylon 6/Plexar 3 blend system; (□) nylon 6/EVA blend system.

3101 blend system and, also, of the nylon 6/Plexar 3 blend system, is much greater than the elongation at break of the nylon 6 homopolymer, which forms the continuous phase. This phenomenon may be attributable to the existence of an interacting (i.e., overlapping) stress field between the neighboring particles, which can promote yielding and subsequently give rise to necking and cold drawing of the matrix phase.¹³ This synergism in ductility, which is uncommon in heterogeneous polymer blends, was also observed in nylon/ionomer blends.¹⁴ The reason for this synergism is not well understood yet. However, it might have originated from the following factors: (1) interfacial adhesion between the discrete and continuous phases; (2) the matrix yielding induced by the inclusion; (3) the necking and cold-drawing mechanism of the nylon matrix. Note that when little adhesion exists between the constituent components, the interfacial adhesion fails before the matrix phase yields.

Impact Strength and Phase Morphology

The notched Izod impact strength of the blend systems investigated are plotted against the blend composition in Figure 16. It is seen that the impact strength of the nylon 6/CXA 3101 blends increases as the amount of CXA 3101 increases from 20 to 40 wt %, whereas the opposite trend is observed with the nylon 6/Plexar 3 blends, as well as with the nylon 6/EVA blends.

Representative SEM micrographs of the fracture surface of the blend systems investigated are shown in Figures 17–19. For comparison purposes, an SEM micrograph of the fracture surface of nylon 6 is also shown in Figure 17. It is seen in these figures that, similarly to the SEM micrographs

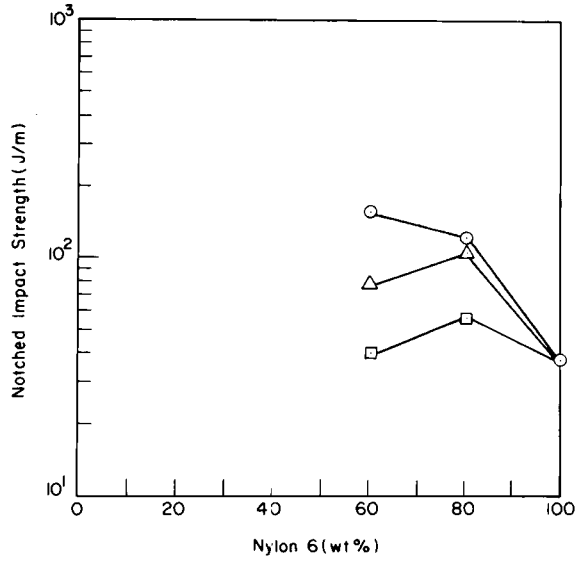


Fig. 16. Izod impact strength vs. blend composition for: (○) nylon 6/CXA 3101 blend system; (△) nylon 6/Plexar 3 blend system; (□) nylon 6/EVA blend system.

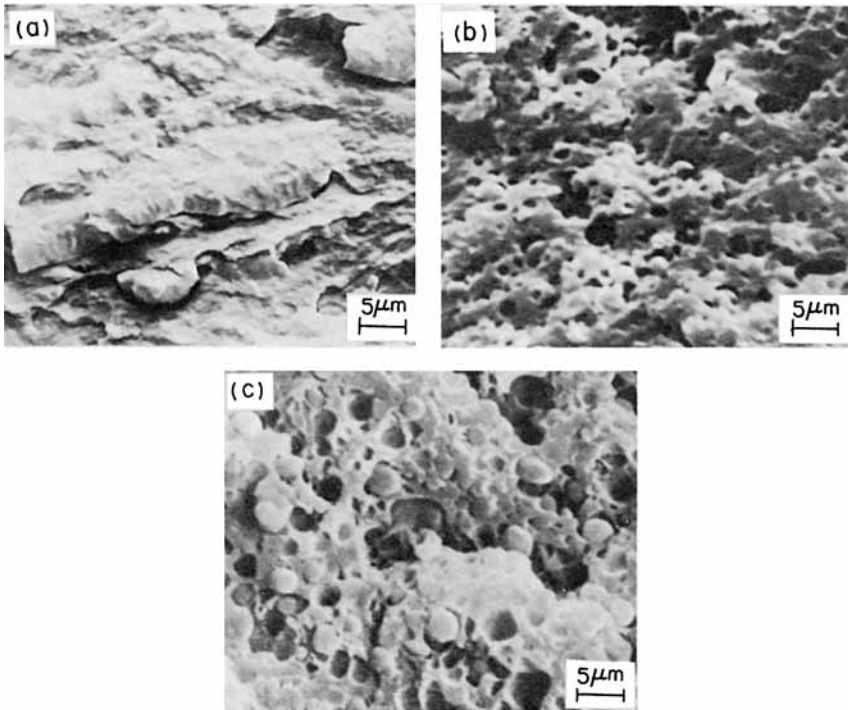


Fig. 17. SEM micrographs of the Izod impact fracture surface of: (a) nylon 6; (b) nylon 6/CXA 3101 = 80/20; (c) nylon 6/CXA 3101 = 60/40.

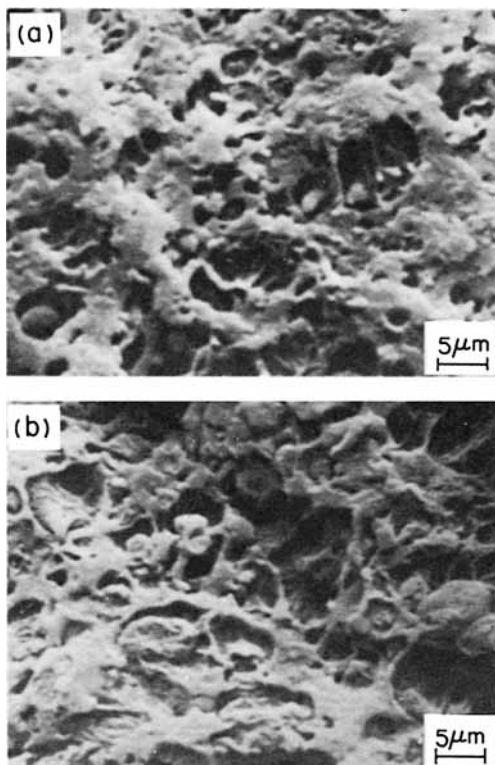


Fig. 18. SEM micrographs of the Izod impact fracture surface of: (a) nylon 6/Plexar 3 = 80/20; (b) nylon 6/Plexar 3 = 60/40.

of the tensile fracture surface shown in Figures 11–13, the domain size of the EVA particles in the nylon 6/EVA blends is very large, compared to that in the nylon 6/CXA 3101 blends or nylon 6/Plexar 3 blends, and that the CXA 3101 particles in the nylon 6/CXA 3101 blends (and, also, the Plexar 3 particles in the nylon 6/Plexar 3 blends) appear to have been covered by a layer of the graft copolymer formed by chemical reactions between the carboxyl or anhydride groups present in the CXA 3101 or in the Plexar 3 and the amino end groups of the nylon 6. This argument is based on the discussion presented in Part I of this series.⁴ Note in Figure 19 that many broken EVA particles are seen.

In the past, various theories have been proposed to explain the toughening of brittle polymer with rubber inclusions.^{15–24} They are: (1) rubber energy absorption¹⁶; (2) crack branching induced by rubber particles¹⁷; (3) energy absorption by yielding of the matrix and the ductility induced by strain dilatation near the rubber inclusions^{18–20}; (4) matrix yielding.^{21–24} Depending on the material dealt with, each of the above toughening mechanisms may make a different contribution to the rubber-toughening effect. Particularly noteworthy is the recent study by Wu,¹⁵ who investigated the impact fracture mechanisms of rubber-toughened nylon 66, by measuring the energy dissipated in several different processes in notched fracture and by pre-

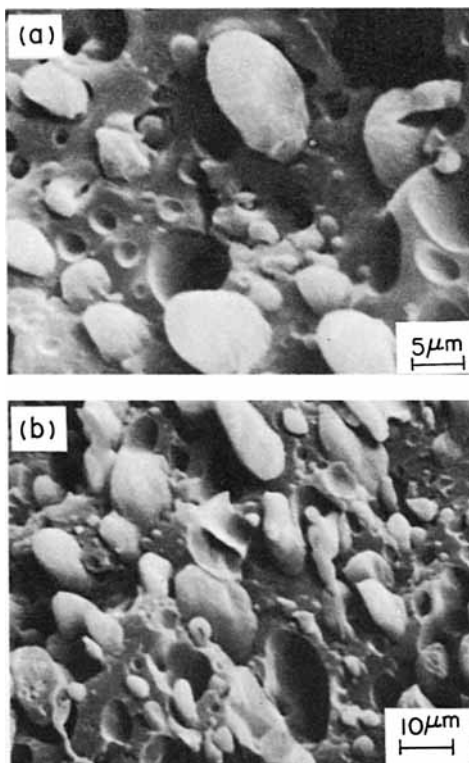


Fig. 19. SEM micrographs of the Izod impact fracture surface of: (a) nylon 6/EVA = 80/20; (b) nylon 6/EVA = 60/40.

senting an energy balance. Wu¹⁵ pointed out that, when rubber particles are not exposed at all on the crack surface, the impact fracture mechanism, which postulates that the impact energy is absorbed as strain energy by the rubber particles, is not applicable. The SEM micrographs presented by Wu are very similar in appearance to those of the nylon 6/CXA 3101 blend systems shown in Figures 8, 11, and 17.

Before closing, one should mention a most interesting study reported very recently by Cimmino et al.,²⁵ who modified an amorphous random ethylene-propylene rubber copolymer (EPDM) by grafting maleic anhydride, and investigated the morphology and tensile/fracture behavior of blends of nylon 6 with the chemically modified EPDM. Although the chemical structure of their modified EPDM is different from that of the CXA 3101 employed in our investigation, many of their experimental observations (namely, tensile properties, impact strength, and SEM micrographs of fracture surface) and conclusions are very similar to those we have presented above in this study.

The authors wish to acknowledge that Werner and Pfleiderer Corp. prepared the polymer blends employed in this study, the American Enka Co. supplied the nylon 6 resin, DuPont Co. supplied the CXA 3101 and EVA resins, and the Chemplex Co. supplied the Plexar 3 resin.

References

1. C. D. Han, *Multiphase Flow in Polymer Processing*, Academic, New York, 1981.
2. C. D. Han and Y. W. Kim, *J. Appl. Polym. Sci.*, **18**, 2589 (1974).
3. H. K. Asar, M. B. Rhodes, and R. Salovey, in *Multiphase Polymers*, S. L. Cooper and G. M. Ester, Eds., Adv. Chem. Ser. No. 176, Am. Chem. Soc., Washington, DC, 1979, p. 489.
4. C. D. Han and H. K. Chuang, *J. Appl. Polym. Sci.*, **30**, 2431 (1985).
5. E. H. Kerner, *Proc. Phys. Sci.*, **69B**, 808 (1956).
6. L. E. Nielsen, *Mechanical Properties of Polymer and Composites*, Dekker, New York, 1974.
7. G. Illing, in *Polymer Blends: Processing, Morphology, and Properties*, E. Martuscelli, R. Palumbo, and M. Kryszewski, Eds., Plenum, New York, 1980, p. 167.
8. K. Fujino, I. Owaga, and H. Kawai, *J. Appl. Polym. Sci.*, **8**, 2147 (1964).
9. M. Takayanagi, S. Eumura, and S. Minami, *J. Polym. Sci., Part C*, **5**, 113 (1964).
10. Z. Hashine and S. Shtrikman, *J. Mech. Phys. Solids*, **11**, 127 (1963).
11. T. Okamoto and M. Takayanagi, *J. Polym. Sci., Part C*, **23**, 597 (1968).
12. T. Kunori and P. H. Geil, *J. Macromol. Sci. Phys.*, **B18**(1), 135 (1980).
13. S. Y. Hobbs, R. C. Bopps, and V. H. Watkins, *Polym. Eng. Sci.*, **23**, 380 (1983).
14. C. R. Lindsey, J. W. Barlow, and D. R. Paul, *J. Appl. Polym. Sci.*, **26**, 9 (1981).
15. S. Wu, *J. Polym. Sci., Polym. Phys. Ed.*, **21**, 699 (1983).
16. E. H. Merz, G. C. Claver, and M. Baer, *J. Polym. Sci.*, **22**, 325 (1956).
17. C. G. Bragaw, in *Multicomponent Polymer Systems*, N. A. J. Platzter, Ed., Adv. Chem. Ser. No. 99, Am. Chem. Soc., Washington, DC, 1971, p. 86.
18. S. Newman and S. Strella, *J. Appl. Polym. Sci.*, **9**, 2297 (1965).
19. S. Newman, in *Polymer Blends*, D. R. Paul and S. Newman, Eds., Academic, New York, 1978, Vol. 2, p. 63.
20. S. Strella, *J. Polym. Sci.*, **4**, 528 (1966).
21. C. B. Bucknall, *Toughened Plastics*, Applied Science, London, 1977.
22. C. B. Bucknall, in *Polymer Blends*, D. R. Paul and S. Newman, Eds., Academic, New York, 1978, Vol. 2, p. 91.
23. J. N. Sultan, R. C. Liable, and F. J. McGarry, *Appl. Polym. Symp.*, **16**, 127 (1971).
24. R. P. Petrich, *Polym. Eng. Sci.*, **12**, 757 (1977).
25. S. Cimmino, L. D'Orazio, R. Greco, G. Maglio, M. Malinconico, C. Mancarella, E. Martuscelli, R. Palumbo, and G. Ragosta, *Polym. Eng. Sci.*, **24**, 48 (1984).

Received August 17, 1984

Accepted October 4, 1984